QED Asymmetry

$e^+e^- \to \mu^+\mu^-$

$$A(\theta) = \frac{\sigma(\theta) - \sigma(\pi-\theta)}{\sigma(\theta) + \sigma(\pi-\theta)}$$

$$= -\frac{2\alpha}{\pi} \ln \tan\frac{\theta}{2} \ln \frac{E}{\Delta E}$$

$$+ \frac{\alpha}{\pi} \frac{1}{1+\cos^2\theta} \times$$

$$\Big[\cos\theta \left(\ln^2 \sin\frac{\theta}{2} + \ln^2 \cos\frac{\theta}{2} \right)$$

$$+ \sin^2\frac{\theta}{2} \ln \cos\frac{\theta}{2} - \cos^2\frac{\theta}{2} \ln \sin\frac{\theta}{2} \Big]$$

R. W. Brown
et al

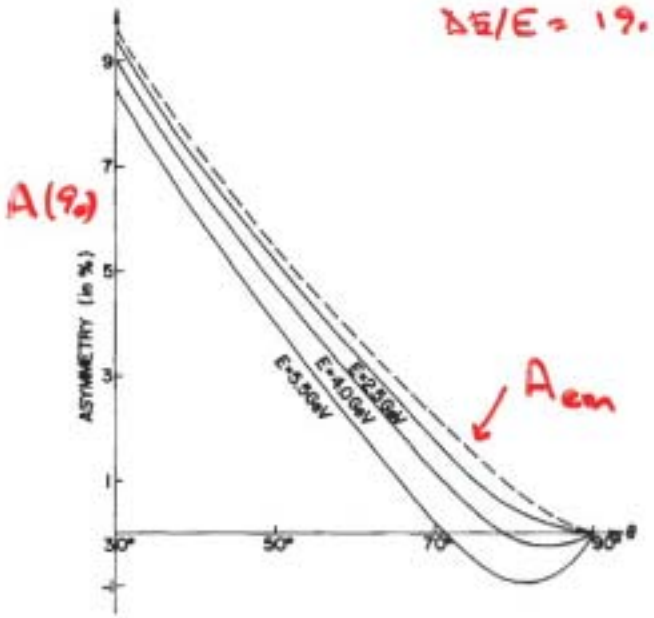

Fig. 2. Asymmetry as a function of θ. We have put $p_+ = -p_- = 0.924, \phi = 0$ (or π), and $\Delta E/E = 1\%$. The dashed line corresponds to A^{EM}, and the solid lines to $(A^{EM}+A^{weak})$ for $E = 2.5$, 4, and 5.5 GeV.

$$A^{weak}(\theta,\phi) = -\frac{1}{f(\theta,\phi)}\frac{\sqrt{2}\,G^F}{\alpha\pi}E^2\cos\theta \qquad (9)$$

where G^F is the Fermi coupling constant (we have taken $E \ll m_z$, where m_z is the mass of the neutral vector boson in this model). We observe that while polarization of the incident beams increases the magnitude of A^{weak}, it slightly decreases A^{EM}. In fig. 2 we plot the sum $A^{EM}+A^{weak}$ for $E = 2.5, 4$, and 5.5 GeV and $p_+ = -p_- = 0.924$.

The large electromagnetic background will make it difficult to separate weak effects by observing only the asymmetry $A(\theta,\phi)$. The lion's share of A^{EM}, arising from the combination of infrared terms in $\delta^B(\mu e)$ and $\delta^{\gamma\gamma}(\mu e)$, can be eliminated by considering the difference

$$\Delta(\theta,\phi,\phi') = A(\theta,\phi) - A(\theta,\phi') \ . \qquad (10)$$

Since Δ^{weak} has the same sign as Δ^{EM}, in general, the sum $\Delta^{EM}+\Delta^{weak}$ could be large enough to be meaningful for experiments. Table 2 contains values for their combined contributions. We describe two experiments which can search for such effects.

Table 2
$\Delta(\theta,\phi,\phi')$ as a function of ϕ' for $\theta = 75°$, $\phi = 0$, $E = 4$ GeV, and $p_+ = -p_- = 0.924$.

ϕ'	Δ^{EM} in %	$\Delta^{weak}+\Delta^{EM}$ in %
30°	−0.4	−1.0
60°	−0.5	−1.4
90°	−0.6	−1.5

Exp.1: In this case one observes one muon and its charge with a momentum uncertainty arising from the finite energy resolution. The terms δ_{sym} are seen in table 2 to be large $\approx -35\%$ and for this reason it is important to include estimates of δ_{sym} in any asymmetry discussion. In the present case contributions of $O(\alpha^2)$ to the asymmetries are important and one must also calculate terms of the same order arising from $\delta^{\gamma\gamma}(\mu e)$ and $\delta^B(\mu e)$. Such terms have not been calculated yet.

Exp. 2: A more relevant experiment is one in which the muons are detected back to back with attendant uncertainties in both collinearity and energy. All our calculations again hold, except for the bremsstrahlung terms, which are now quite different. A recent calculation [11] of the bremsstrahlung terms indicates that their contribution to $|\delta_{sym}|$ is less than 6% for $0.5 \leqslant E \leqslant 5.0$ GeV and a maximum acollinearity of 10°. Under such conditions it seems that a calculation of the asymmetries A and Δ to $O(\alpha)$ is sufficient, and the values of table 2 hold. Finally, since every experiment has its own intrinsic uncertainties, with regard to acollinearity and energy resolution, it is necessary to recalculate only the bremsstrahlung terms for each specific case.

We would like to point out that tin the absence of weak effects a measurement of the asymmetry would constitute an important check of QED. For hadronic final states the polarization of the beams is useful in separating the structure functions. Encouraged by a large asymmetry in this process, one may also look for it in hadronic channels, e.g., $e^+e^- \to \pi^+\pi^-$.

We wish to thank D.B. Cline and A.K. Mann for discussions about the experimental aspects of this problem. Two of us (R.W.B. and E.A.P.) wish to express our appreciation to the Aspen Center for Physics where part of this work was performed.

Central Topic of QCD

$$e^+e^- \to N\bar{N}$$

Remarkable Features of $e^+e^- \to p\bar{p}$, $\bar{p}p \to e^+e^-$

↑ LEAR, FNAL, Future GSI

* Sharp rise at threshold ($s = 4M_p^2$)

→ "baryonium" resonance at $s = 3.5\ \text{GeV}^2$?

* dip in $\sigma(e^+e^- \to 6\pi)$ at $s = 3.5\ \text{GeV}^2$!

Fenice, DM2, FS

analogy: $e^+e^- \to \mu^+\mu^-$ true moonium below threshold and $\frac{1}{R}$ above

* $\sigma(e^+e^- \to n\bar{n}) > \sigma(e^+e^- \to p\bar{p})$!

⇒ Need $e^+e^- \to \Lambda\bar{\Lambda}, \Sigma\bar{\Sigma}, \Delta\bar{\Delta}, N\Delta, \ldots$

\+ Polarization measurements to determine phases

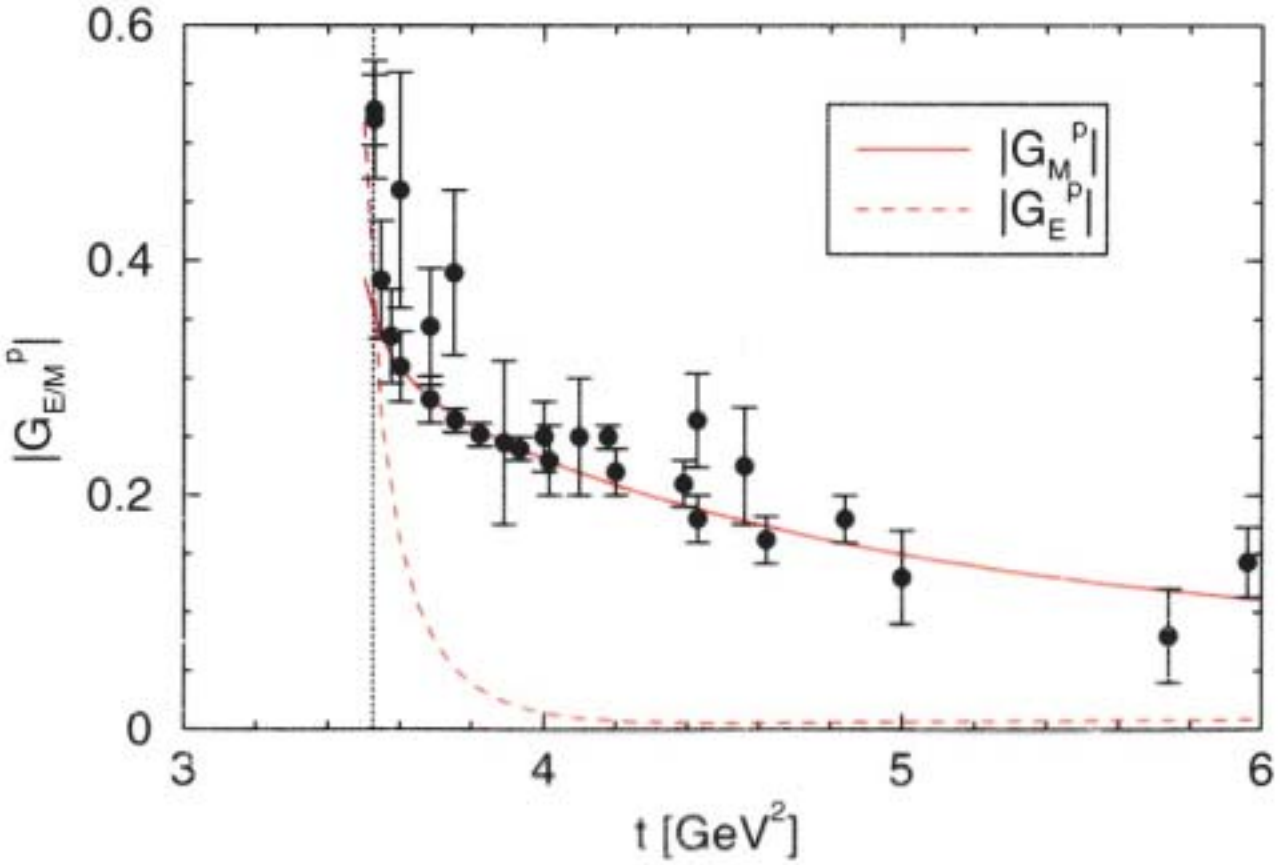
0.6
0.4
0.2
0
3
4
5
6
$|G_{E/M}^{p}|$
t [GeV^2]
$|G_M^p|$
$|G_E^p|$

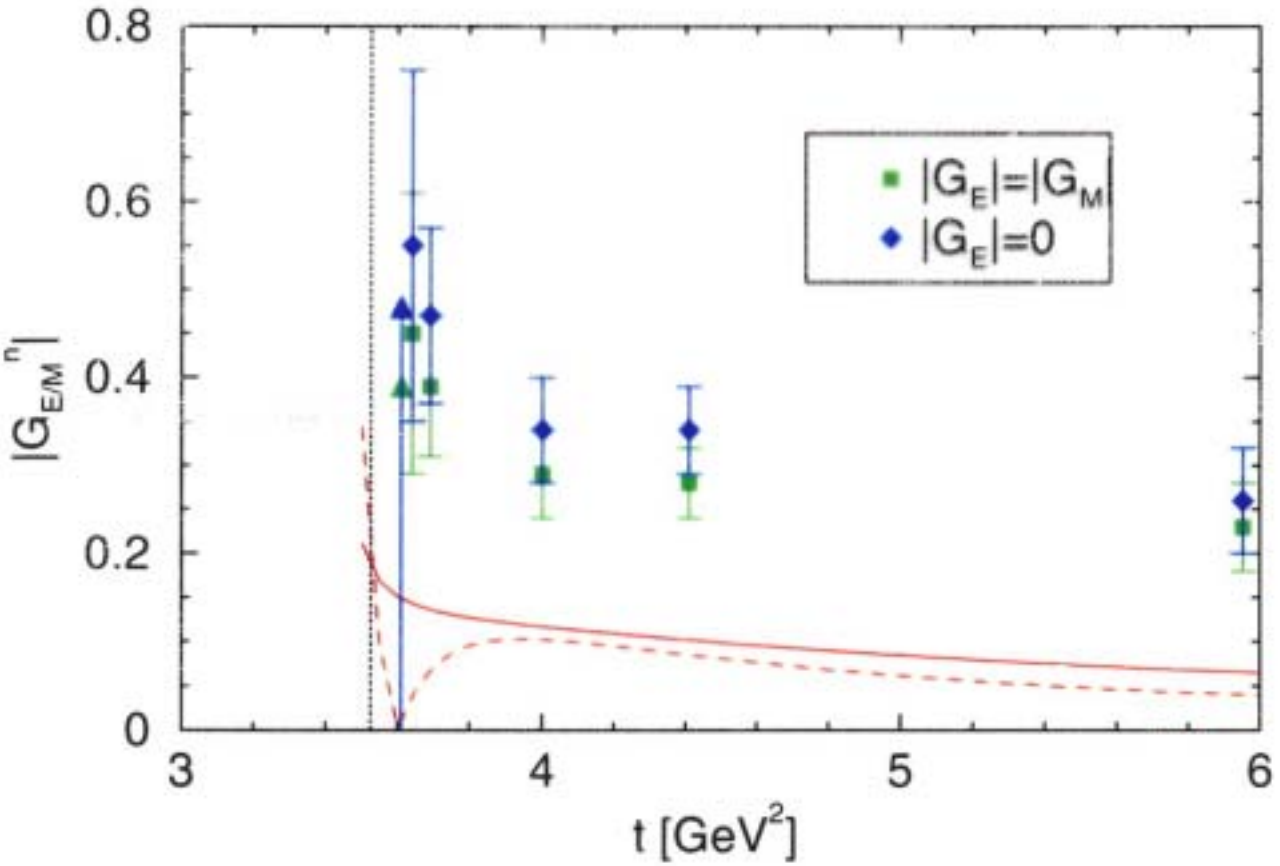
0.8
0.6
0.4
0.2
0
3
4
5
6
$|G_{E/M}^{n}|$
t [GeV^2]
$|G_E|=|G_M|$
$|G_E|=0$

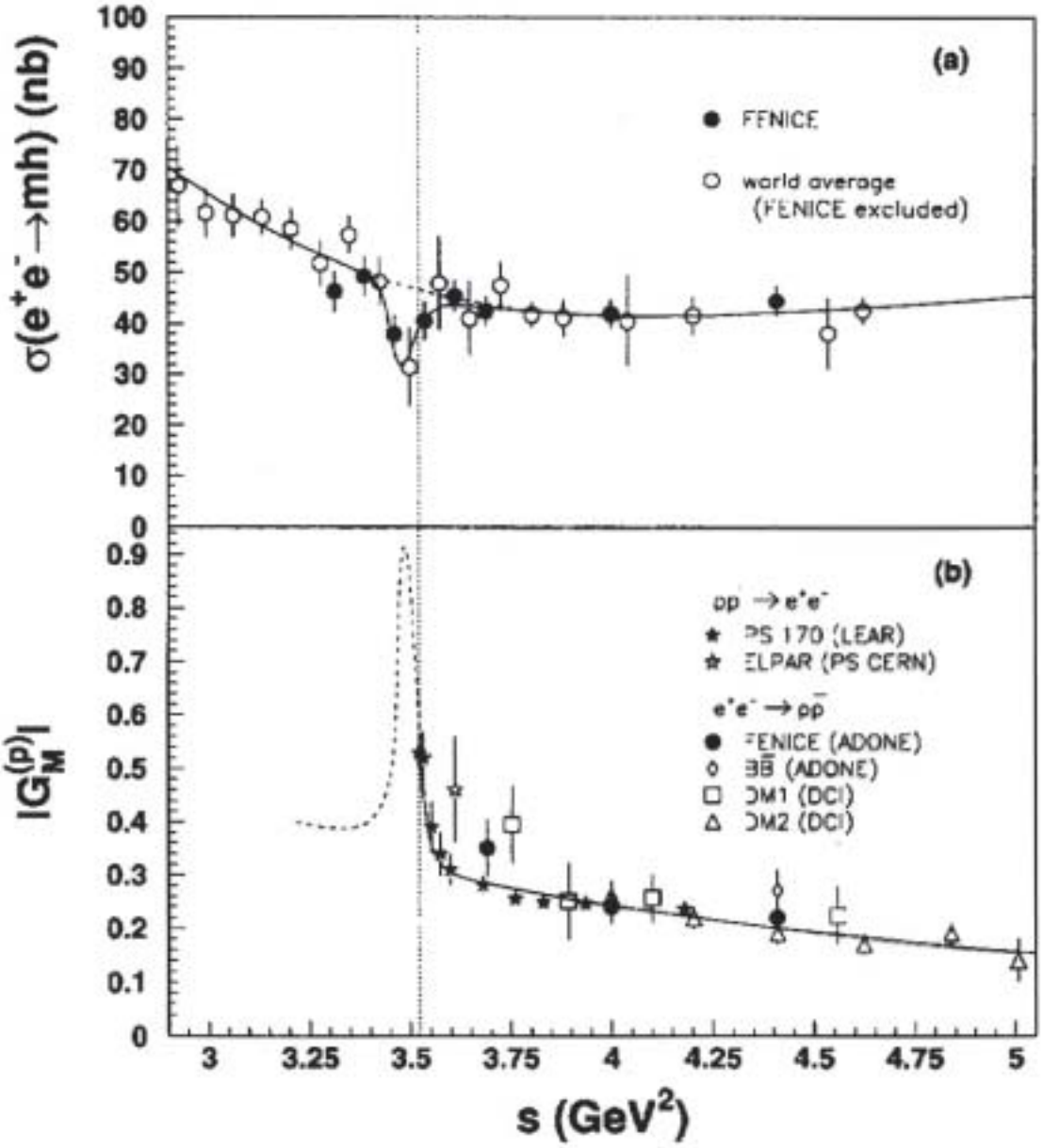

Multihadronic cross-section (upper plot) and proton form factor (lower plot) as a function of the center of mass energy. A combined fit is also shown.

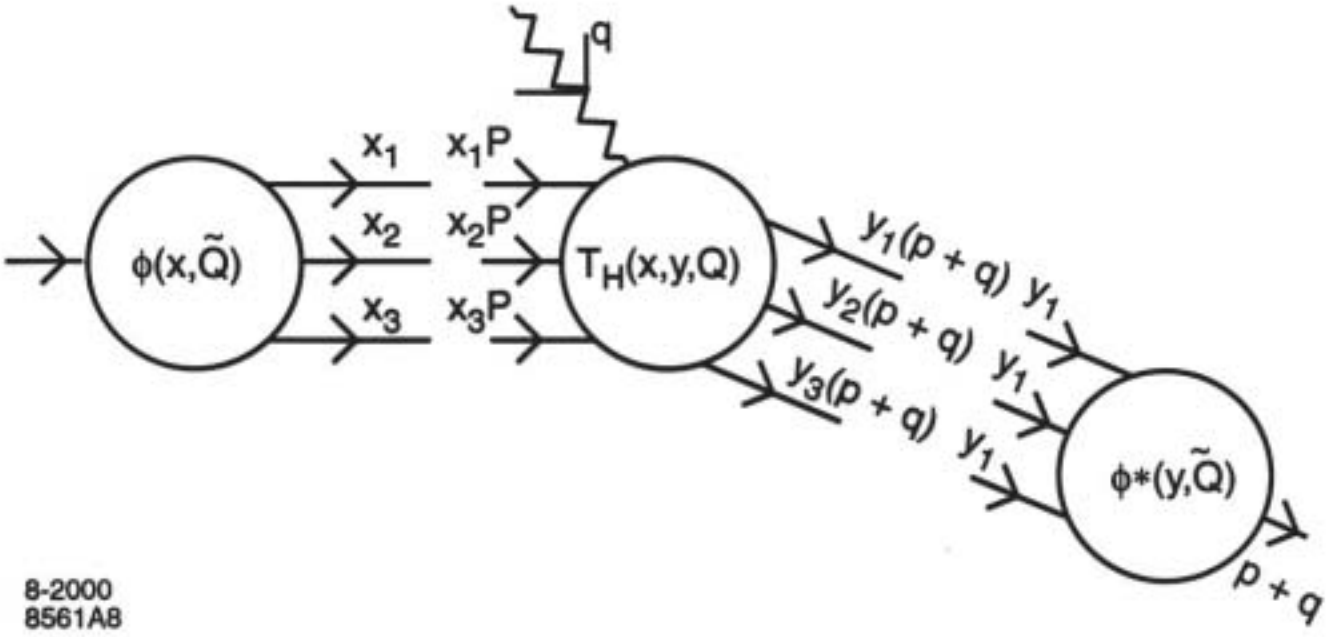

8-2000
8561A8

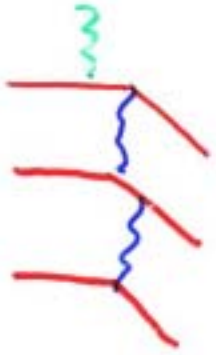

$$\frac{\alpha_s^2(Q^*)}{Q^4}$$

high $Q^2 = -q^2$

$Q^2 \gg \langle k_\perp^2 \rangle$

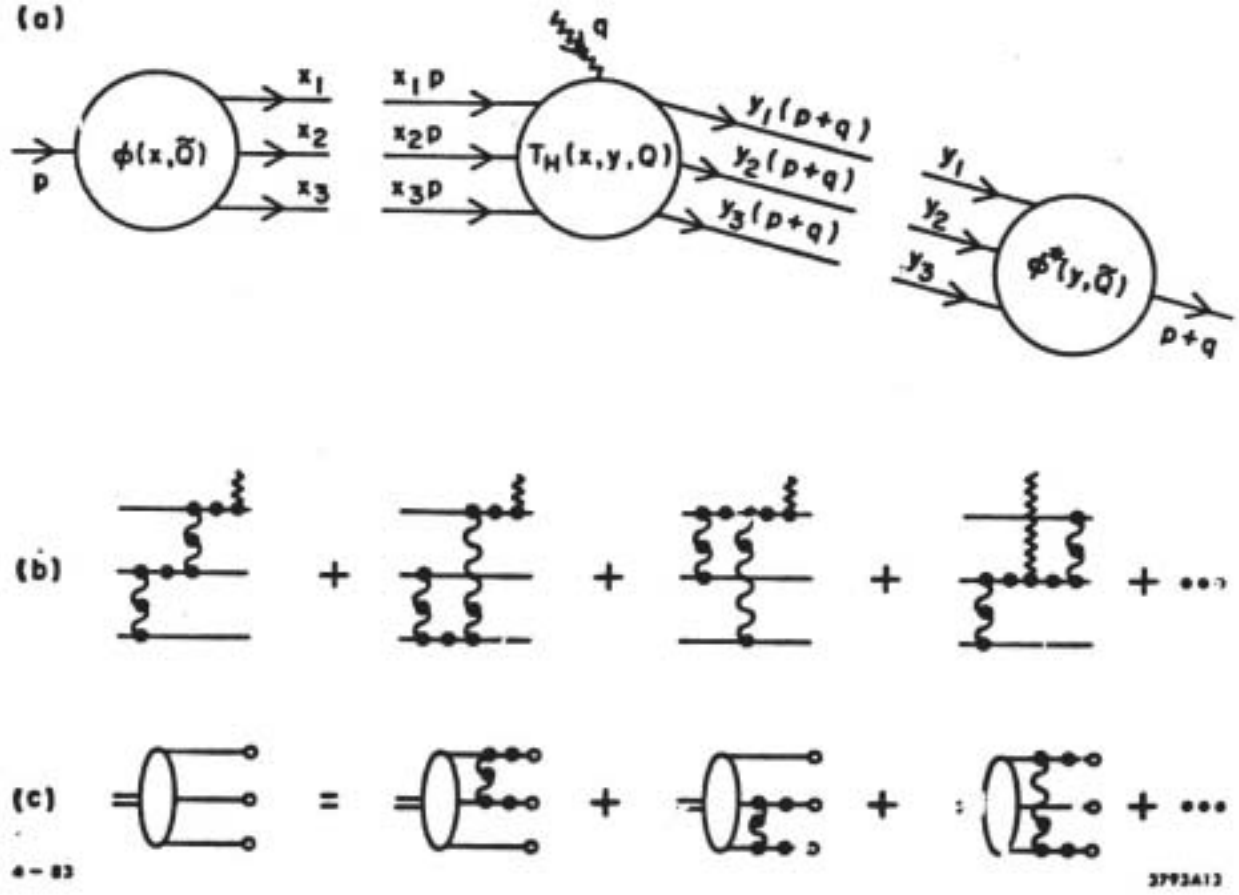

Figure 19. (a) Factorization of the nucleon form factor at large Q^2 in QCD. (b) The leading order diagrams for the hard scattering amplitude T_H. The dots indicate insertions which enter the renormalization of the coupling constant. (c) The leading order diagrams which determine the Q^2 dependence of the distribution amplitude $\phi(x,Q)$.

Calculation of proton form factor in PQCD

Lepage + SJB
Chernyak + Zhitnitsky
Radyushkin
Muller + Dorokhov

Feynman endpoint: Isgur et al

Calculation of Proton Form Factor in QCD at high Q^2

Factorization

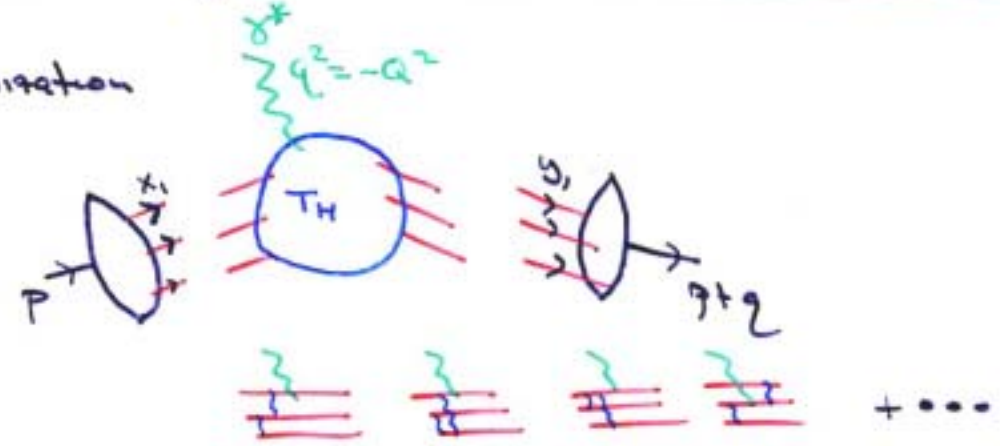

G.P. Lepage SJB

Chernyak + Zhitnitsky

$\alpha(Q^2 \to 0)$ → const. avoids singularity

$$F_1(Q^2) = \int_0^1 dy_i \int_0^1 dx_i \; \phi^*(y_i, \breve{Q})\, T_H(x_i, y_i, Q)\, \phi(x_i, \breve{Q})$$

$$T_H = \frac{\alpha_s^2(\breve{Q}^2)}{Q^4} f(x_i, y_i) \left[1 + O\left(\frac{\alpha_s}{\pi}\right)\right]$$

"Distribution Amplitude"

$$\phi(x_i, \breve{Q}) = \int d^2k_{\perp i}\; \Psi_{qqq}(x, k_\perp)\; \theta(k_{\perp i}^2 < \breve{Q}^2)$$

$\phi(x_i, \mu \sim 1\,\text{GeV})$ determined from QCD Sum Rules

$$\phi(x_i, Q) = x_1 x_2 x_3 \sum_{n \geq 0} a_n(\breve{Q}^2) \left(\ln \frac{\breve{Q}^2}{\Lambda^2}\right)^{-\gamma_n}$$

$$F_1(Q^2) = \frac{\alpha_s^2(\breve{Q}^2)}{Q^4} \sum_{n,m} d_{nm} \left(\ln \frac{\breve{Q}^2}{\Lambda^2}\right)^{-\gamma_n - \gamma_m}$$

corrections : higher order in α_s, m/Q.

Fig from Arnold et al

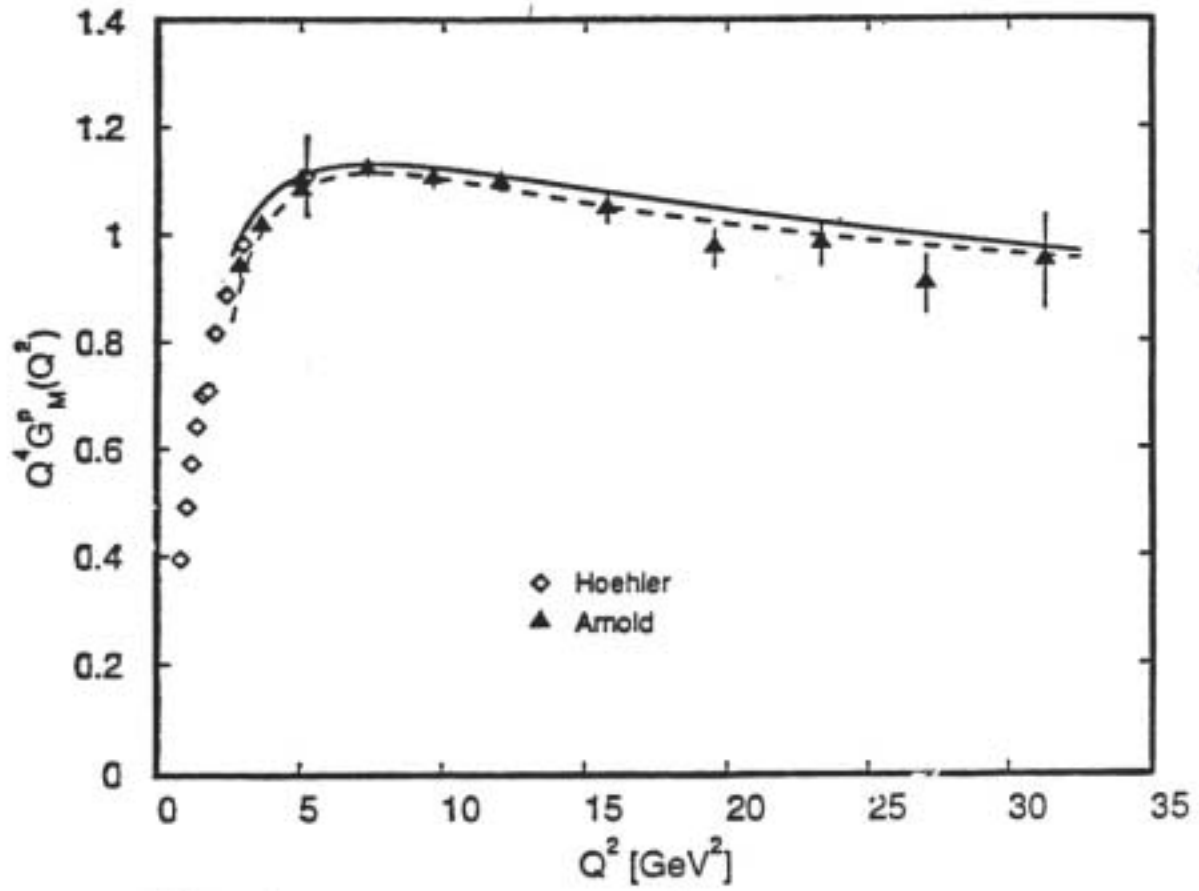

$\sim \alpha_s^2(Q^2)$

Fig. 4

PQCD predicts $\frac{1}{Q^4}$!

Consistent with $F_1(Q^2) \sim \frac{\alpha_s^2(Q^2)}{Q^4}$

Karll, Pilsner,
Schürmann, Schwarz

$q + \bar{q}q$

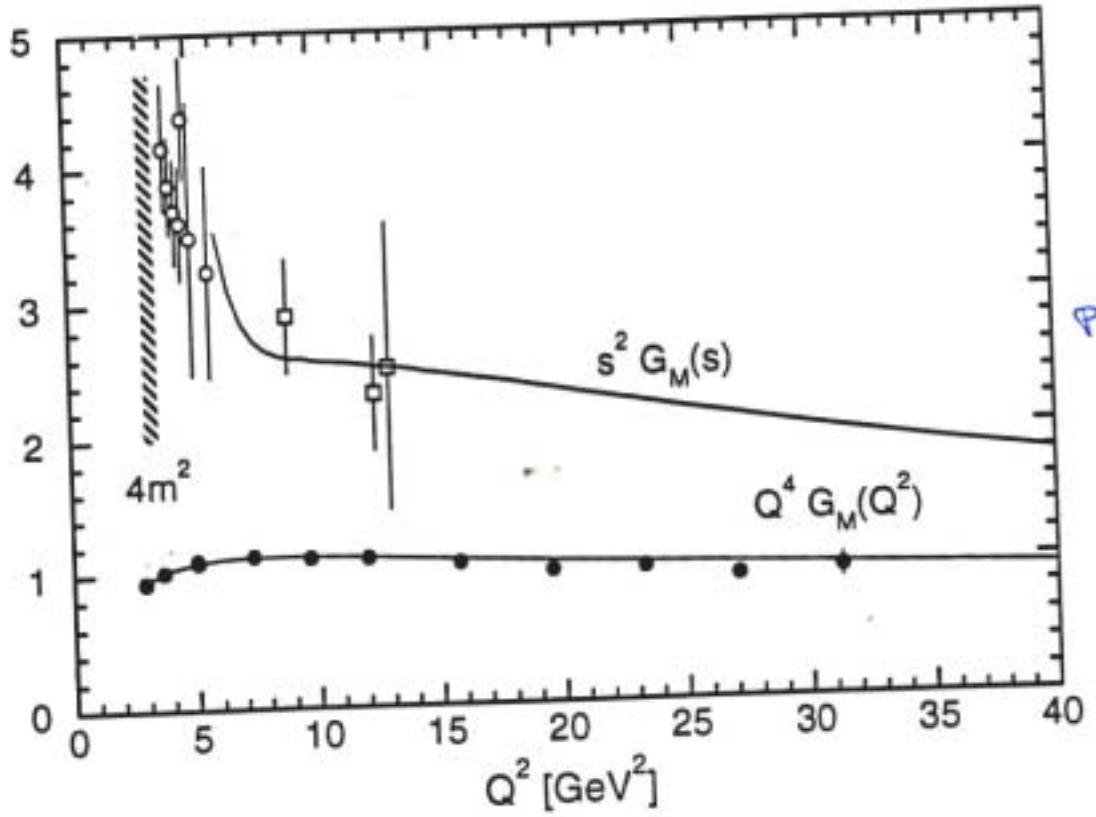

$p\bar{p} \to l^+ l^-$
E760

Fig. 1

Ji, Pang, Robertson, SJB:

Little room
for variation
$\eta_b \alpha_V\left(\frac{Q^2}{9}\right)$!

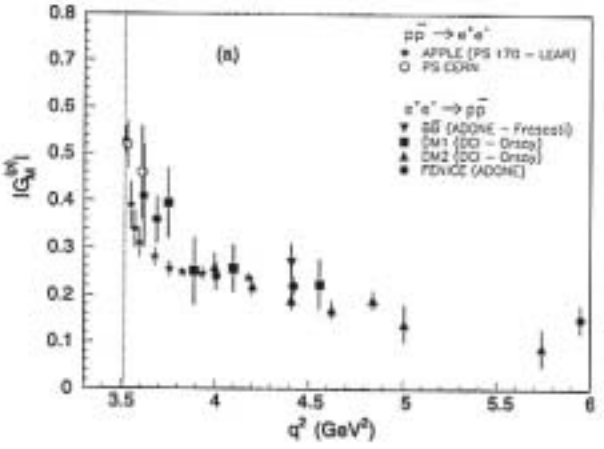

The proton magnetic form factor versus q^2: the low energy region.

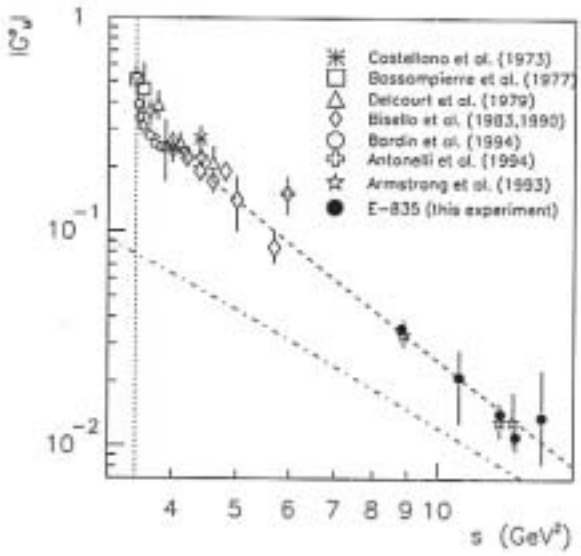

The proton magnetic form factor versus q^2. The dashed and dot-dashed curves are explained in the text.

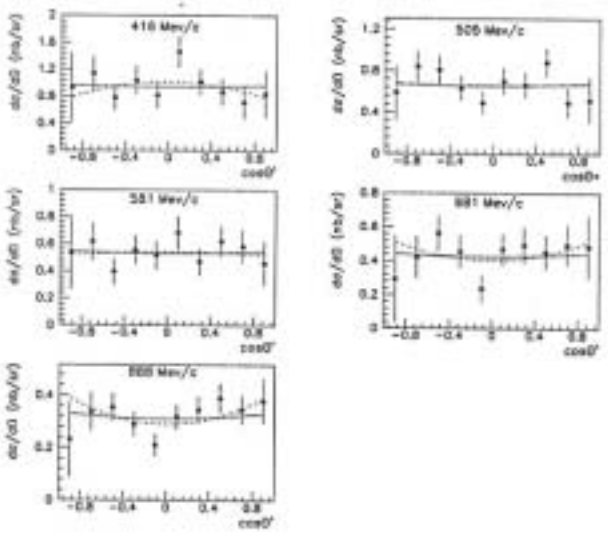

Differential cross sections for $p\bar{p} \to e^+e^-$ events from PS170 experiment. The full line is the fit of data with $|G_E^p| = |G_M^p|$. The dashed line fits the data with indipendent $|G_M^p|$ and $|G_E^p|/|G_M^p|$.

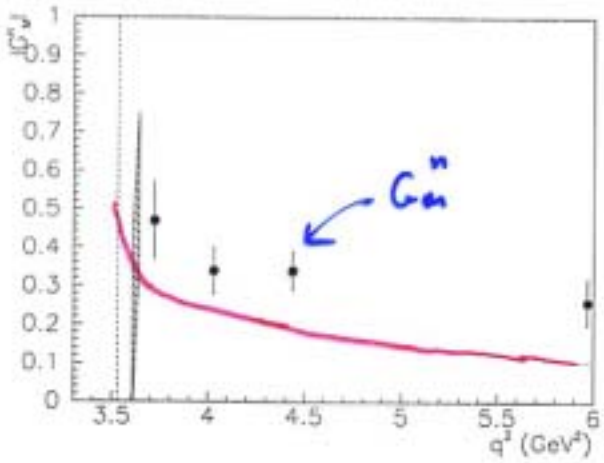

The neutron magnetic form factor versus q^2. The dotted line is a parameterization of the proton FF.

Analyticity + Crossing of Form Factors

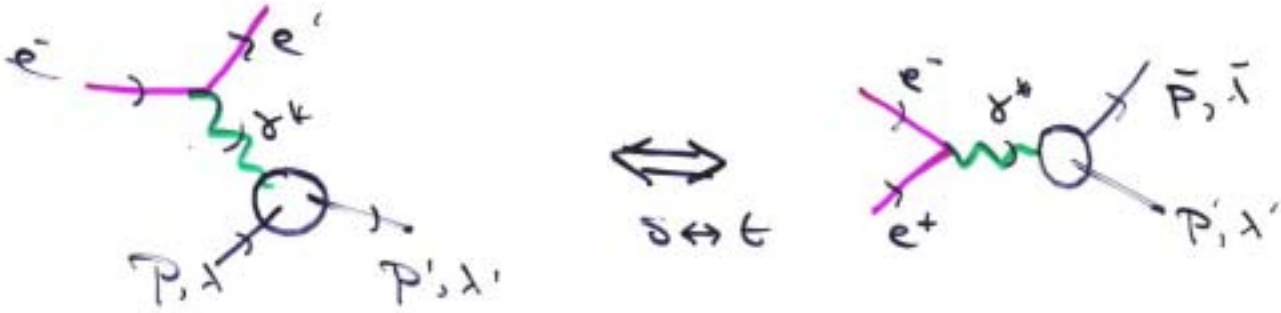

real form factors — complex form factors

$$q^2 = (p' - p)^2 < 0 \qquad q^2 = (\bar{p} + p')^2 > 0$$

- Single function $F_i(q^2)$ for positive, negative q^2
- same power-law fall off at large (q^2)
- Dispersion relation

$$F_i(q^2) = F_i(0) - \frac{q^2}{\pi} \int_{4m_p^2}^{\infty} ds \, \frac{\mathrm{Im}\, F_i(s)}{s\,(s - q^2 + i\epsilon)}$$

and others

- Can construct $F_i(q^2)$ in unphysical regime $0 < q^2 < 4m_p^2$.

resonances

Use $G_E = G_M$ at $q^2 = 4m_p^2$.

Belushkin et al

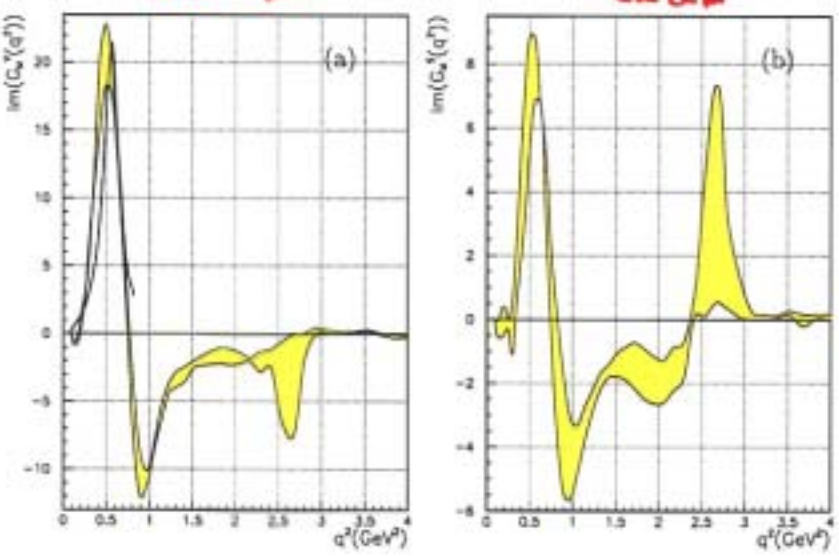

Fig. 5a,b. Imaginary part of the nucleon magnetic isovector **a** and isoscalar **b** form factor. Expectation from unitarity relation is also shown in **a**

way by means of a DR for $\log|G(Q^2)|$, using space-like and time-like data together with a regularization method.

Resonances have been found to be consistent with the $\rho(770)$ and $\rho'(1600)$ masses. However, a very large ρ width is obtained. This result is reminiscent models in which mesons are different from baryons. No evidence has been found for a sizeable Φ contribution: this is contrary to what is expected if there is indeed a large polarized strange content in the nucleon. This work, which aims toward the understanding of the sources of the discrepancies between our conclusions and other dispersion analyses, as well as evaluations by means of the unitarized VDM, is in progress.

Acknowledgements. We warmly acknowledge the FENICE Collaboration and D. Drechsel, U. Meißner, and M. Karliner for their important remarks.

References

1. M.Gourdin, Phys. Rep. 11, No. 2 (1974) 29.
2. J.S.Ball, D.Y.Wong Phys. Rev. 130 (1963) 2112; M.W.Kirson Phys. Rev. 132 (1963) 1249; J.S.Levinger, C.P.Wang, Phys. Rev. 136 (1964) B733; J.S.Levinger, C.P.Wang, Phys. Rev. 138 (1965) B1207; B.Orman, Phys. Rev. 138 (1965) B1308; B.Orman, Phys. Rev. 145 (1966) 1140.
3. G.F.Chew et al., Phys. Rev. 110 (1958) 265; P.Federbush, M.L.Goldberger, S.B.Treiman, Phys. Rev. 112 (1958) 642; S.D.Drell, F.Zachariasen, E.m. Structure of Nucleons (Oxford Univ.Press, Oxford, 1960); J.S.Levinger, R.F.Peierls, Phys. Rev. 134 (1964) B1314; G.L.Kane, R.A.Zdanis, Phys. Rev. 151 (1966) 1239; F.Chilton, F.J.Uhrhane, Bull. Am. Soc. 11 (1966) 396;
4. R.Gatto, N.Cabibbo, Phys. Rev. 124 (1961) 1577; V.Wataghin, Nucl. Phys. B10 (1969) 107; J.C.Korner, M.Kuroda, Phys. Rev. D16 (1977) 2165; P.Cesselli, M. Nigro, C. Voci, Proc. of Workshop on Lear Physics Erice (1982); M.Van Der Velde, M.I.Polikarpov, Jour. Nucl. Phys. 35 (1982) 180; E.Etim, A.Malecki, LNF-89-023 (1989); M.M.Giannini, E.Santopinto, M.I.Krivoruchenko, Proceed. Int. Conf. on Meson and Nuclei at Interm. Energies, Dubna, 1994.
5. S.Dubnička, Nuovo Cimento A104 (1991) 1075; S.Dubnička, A.Z.Dubničkova, P.Strizener Nuovo Cimento A106 (1993) 1253.
6. J.Ellis, M.Karliner, H.Kowalski, Phys. Lett. B235 (1990) 341; G.Holzwarth, Z. Phys. A356 (1996) 339.
7. T.H.R.Skyrme, Nucl. Phys. 31 (1962) 556.
8. G.Höhler et al., Nucl. Phys. B114 (1976) 505.
9. H.W.Hammer, U.G.Meißner, D.Drechsel, Phys. Lett. B385 (1996) 343.
10. A.Z.Dubničkova, presented at the LNF Spring School 1998.
11. H.Forkel, Prog. Part. Nucl. Phys. 36 (1996) 229. P.Mergell, U.-G. Meißner, D. Drechsel, Nucl. Phys. A596 (1996) 367.
12. J.E.Bowcock, W.N.Cottingham, J.G.Williams, Nucl. Phys. B3 (1967) 95.
13. V.Blobel, Lectures given at the 1984 CERN School of Computing; A.Höcker, V.Kartvelishvili, MC-TH-95/15, LAL-95/55; E.T.Janes, Proc. IEEE 70 (1982) 939; S.F.Gull, J.Skilling, Proc. IEEE 131 (1984) 1; J.Antolin, A.Cruz, Journ. Math. Phys. 27 (1986) 104.
14. G.Bassompierre et al., Phys. Lett. B68 (1977) 477; B.Delcour et al., Phys. Lett. B86 (1979) 395; D.Bisello et al., Z. Phys. C48 (1990) 23; T.A.Armstrong et al., Phys. Rev. Lett. 70 (1992) 1212; A.Antonelli et al, Phys. Lett. B334 (1994) 431; E835 coll., presented at Hadron97 (August 1997).
15. G.Bardin et al., Nucl. Phys. B411 (1994) 3.
16. A.Antonelli et al, Phys. Lett. B313 (1993) 283; A.Antonelli et al., Nucl. Phys. B517 (1998) 3.
17. V.L.Chernyak, A.R.Zhitnitsky, Nucl. Phys. B246 (1984) 52.
18. S.J.Brodsky, Nucleon Structure Workshop (Frascati, October 1988); T.Hyer, Phys. Rev. D47 (1993) 3875.

Analytic properties of Form Factors

$$Q_I = Q_I(x_i, m^2)$$

Compute Form factors from overlap of LFWFs

$q^+ = 0$
$q^2 = -q_\perp^2$

$$m^2 = \sum_i \frac{k_{\perp i}^2 + m_i^2}{x_i} \to \sum_i \frac{\left(k_{\perp i} + (\delta_i - x_i)\, q_\perp\right)^2 + m_i^2}{x_i}$$

$$\Rightarrow \quad F_i(q^2) \sim Q\left(m^2 \sim O(Q^2)\right)$$

$$\sim \left(\frac{1}{Q^2}\right)^n \quad \text{mod log } Q^2$$

Agrees with PQCD analysis — Belitsky, Ji, Yuan

$$\frac{Q^2 F_2(Q^2)}{F_1(Q^2)} \sim \log^2 Q^2$$

not $\dfrac{Q F_2(Q^2)}{F_1(Q^2)} \sim \text{const}$ — Miller, Frank, Coester, Sellumph, Ralston, Kroll

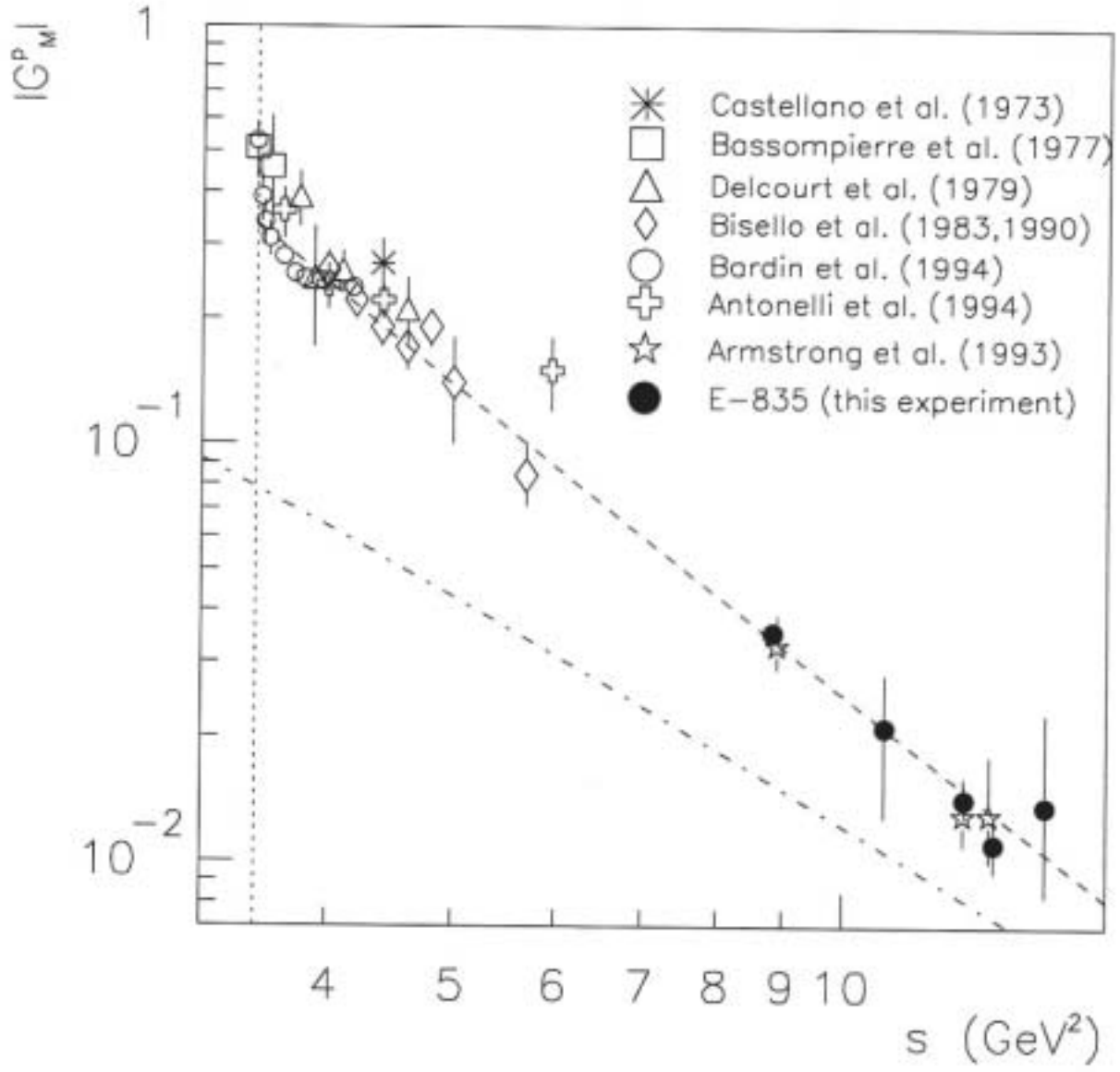

$G_M(s) = \frac{C}{s^2 \ln^2(s/\Lambda^2)}$

dipole

$F_2/F_1 = 0.66/\mathrm{sqrt}[\tau]$

$\tau = Q^2/4m^2$

J. Miller

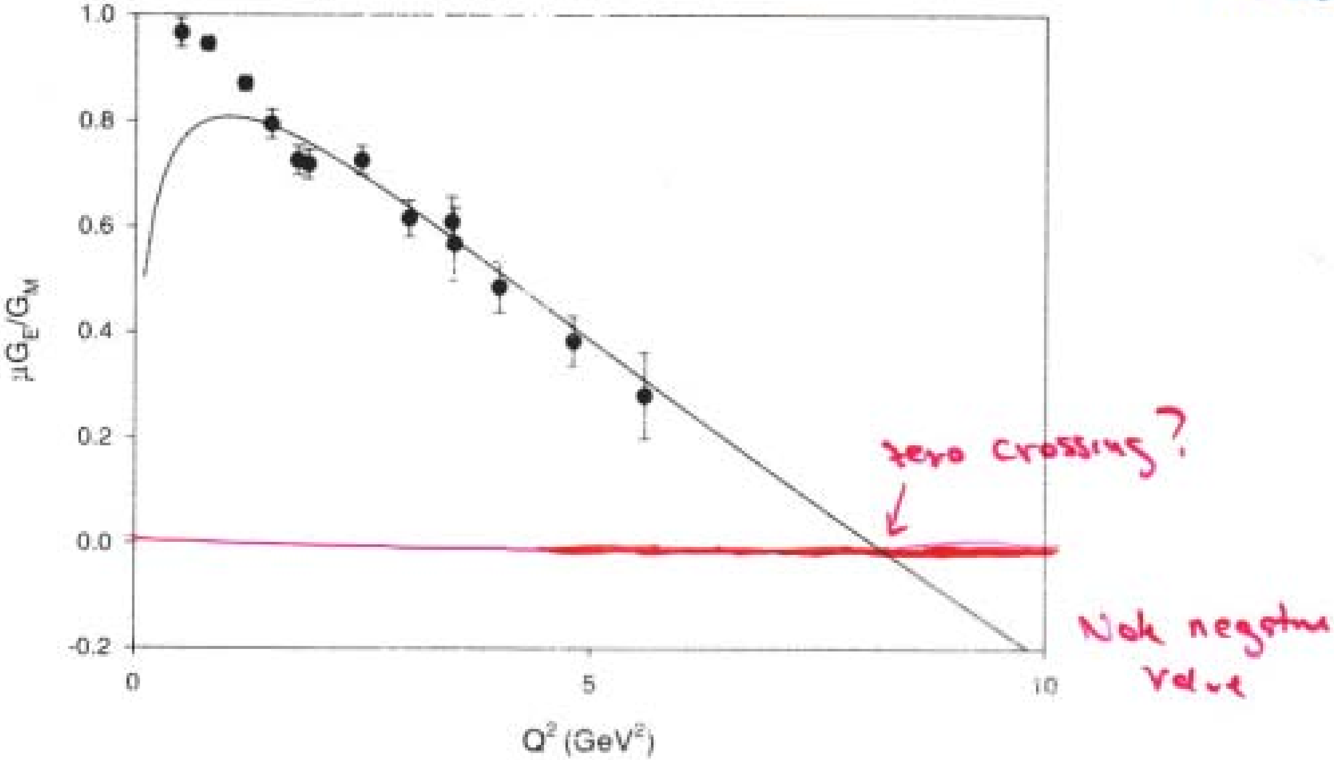

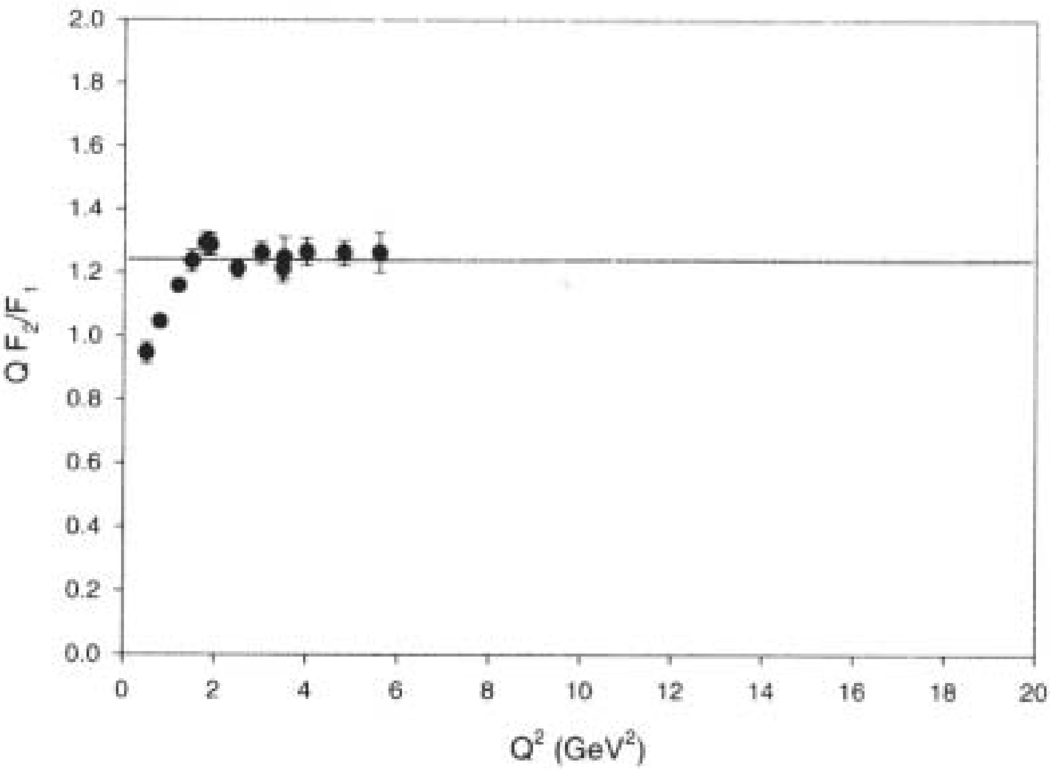

See Miller + Frank

Determination of Relative Phase of Timelike Form Factors

* key measure to settle Rosenbluth vs Spin Transfer

Single-Spin Polarization in $e^+e^- \to p\uparrow \bar{p}$

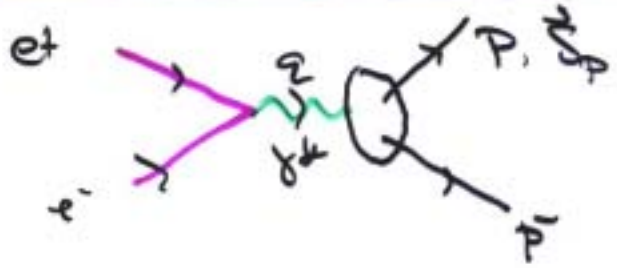

Carbon shell target
Use second scatt to determine S_p

$\tau = q^2/4M_p^2 > 1$

$$P_y = \frac{\sqrt{\tau}\ \sin 2\theta\ \mathrm{Im}\, G_E^* G_M}{\tau |G_M|^2 (1+\cos^2\theta) + |G_E|^2 \sin^2\theta}$$

Dubnicka
Dubnicka
Strunzova
Tkebuchava

Rock

$\hat{S}\cdot(\hat{P}_p \times \hat{k}_e)$ correlation — normal to production plane

$\mathrm{Im}\, G_E^* G_M = (\tau-1)\mathrm{Im}\, F_2^* F_1$

Carlson
Hiller
Mwang
SJB

Various models for $G_E(q^2)$, $G_M(q^2)$ give very different relative phase when analytically continued for $q^2<0$ to $q^2 > 4M_p^2$.

P_x, P_y, P_z ← require P_e →

* $P_y = \sqrt{\tau}\,\dfrac{\sin 2\theta\ \mathrm{Im}\, G_E^* G_M}{D}$

* $P_x = -P_e\,\dfrac{2\sqrt{\tau}\,\sin\theta\ \mathrm{Re}\, G_E^* G_M}{D}$

* $P_z = -P_e\,\dfrac{2\tau\,\cos\theta\,|G_M|^2}{D}$

$D = \tau |G_M|^2 (1+\cos^2\theta) + |G_E|^2 \sin^2\theta$

$\tau = q^2/4M_p^2 \gg 1$

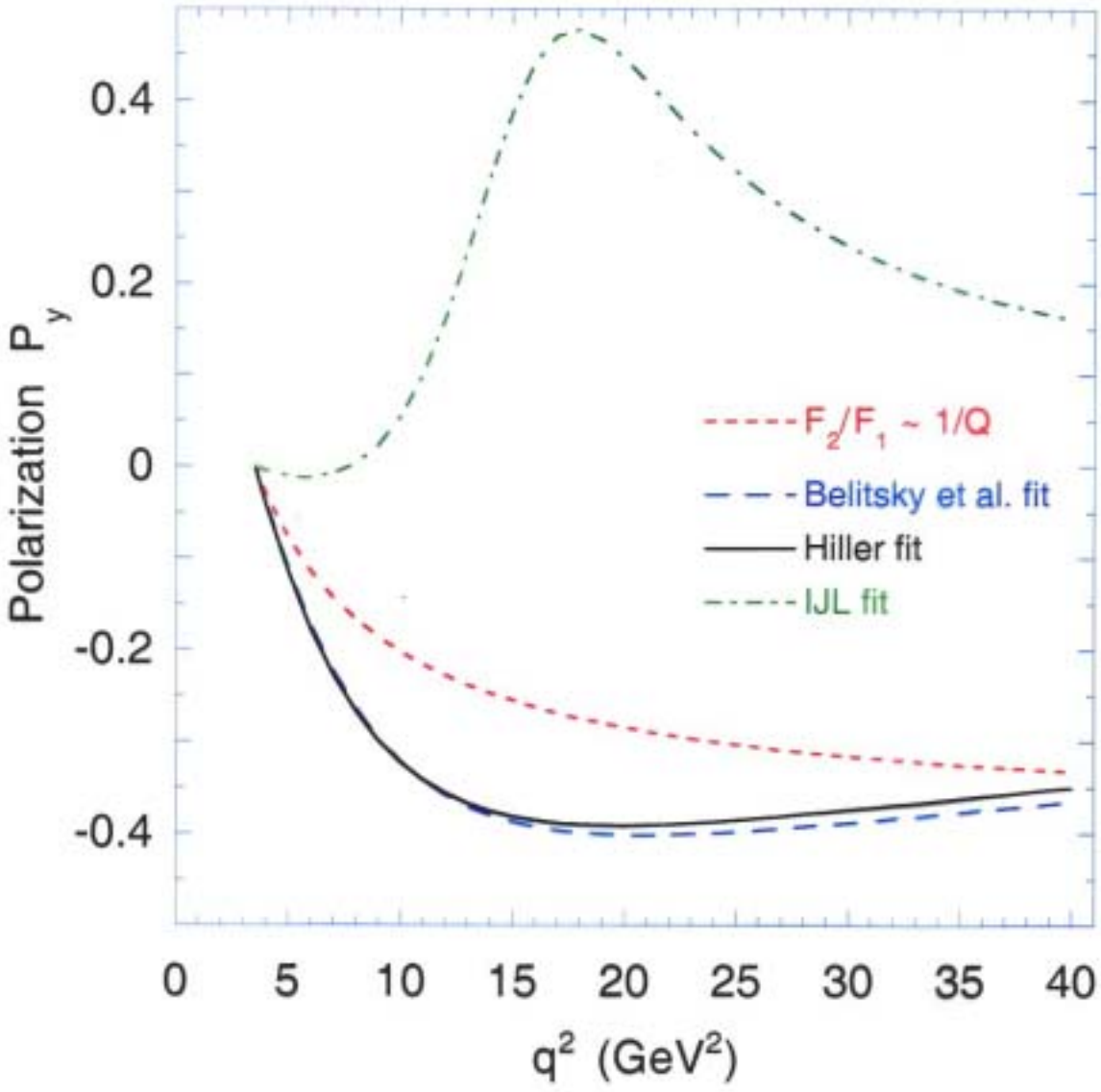

$(\log^2 Q^2)/Q^2$ improved

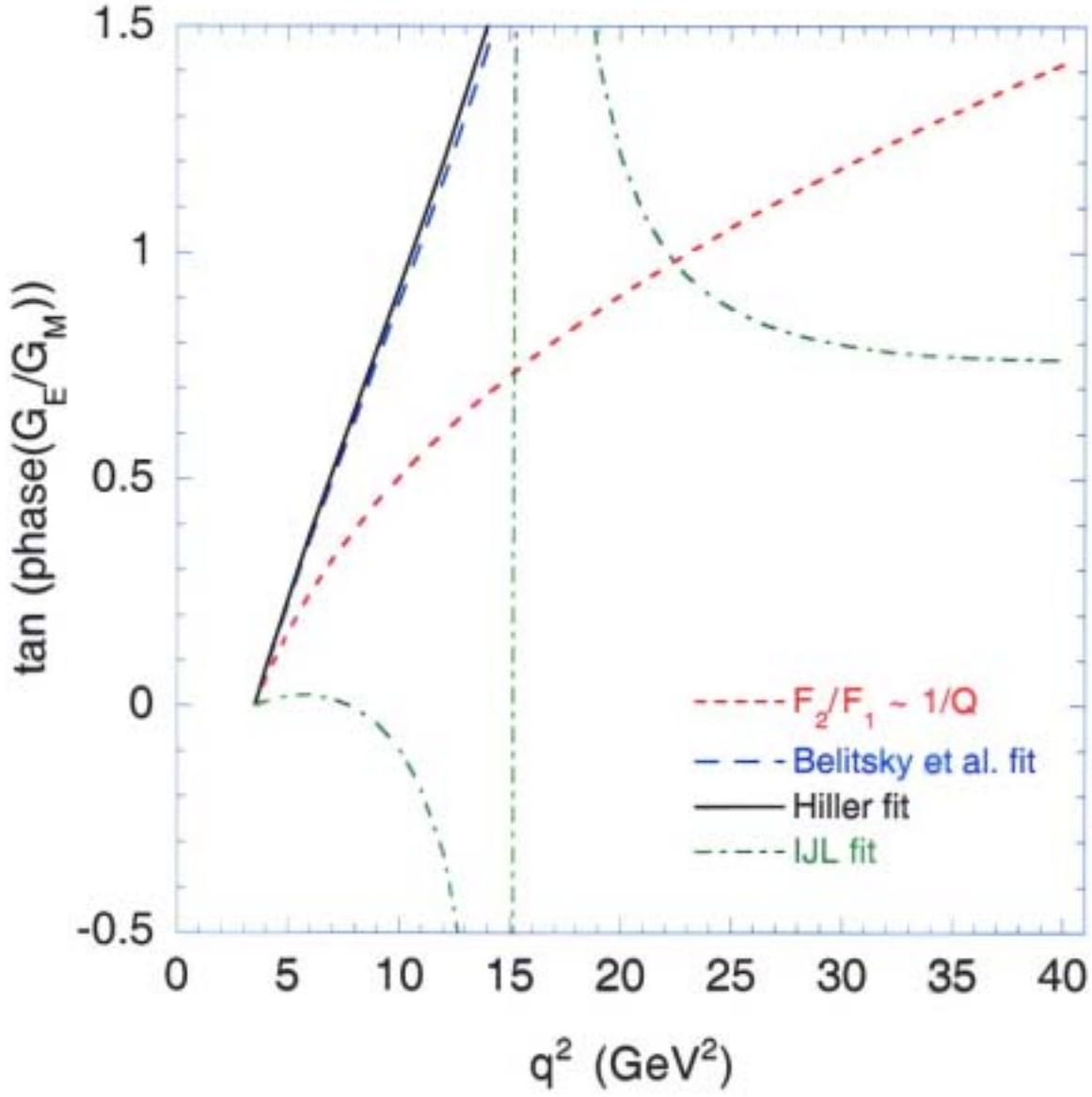

$\log^2 q^2/Q^2$ improved

$\tan(\delta_E - \delta_M)$

Carlson
Hiller
Kwang
SJB

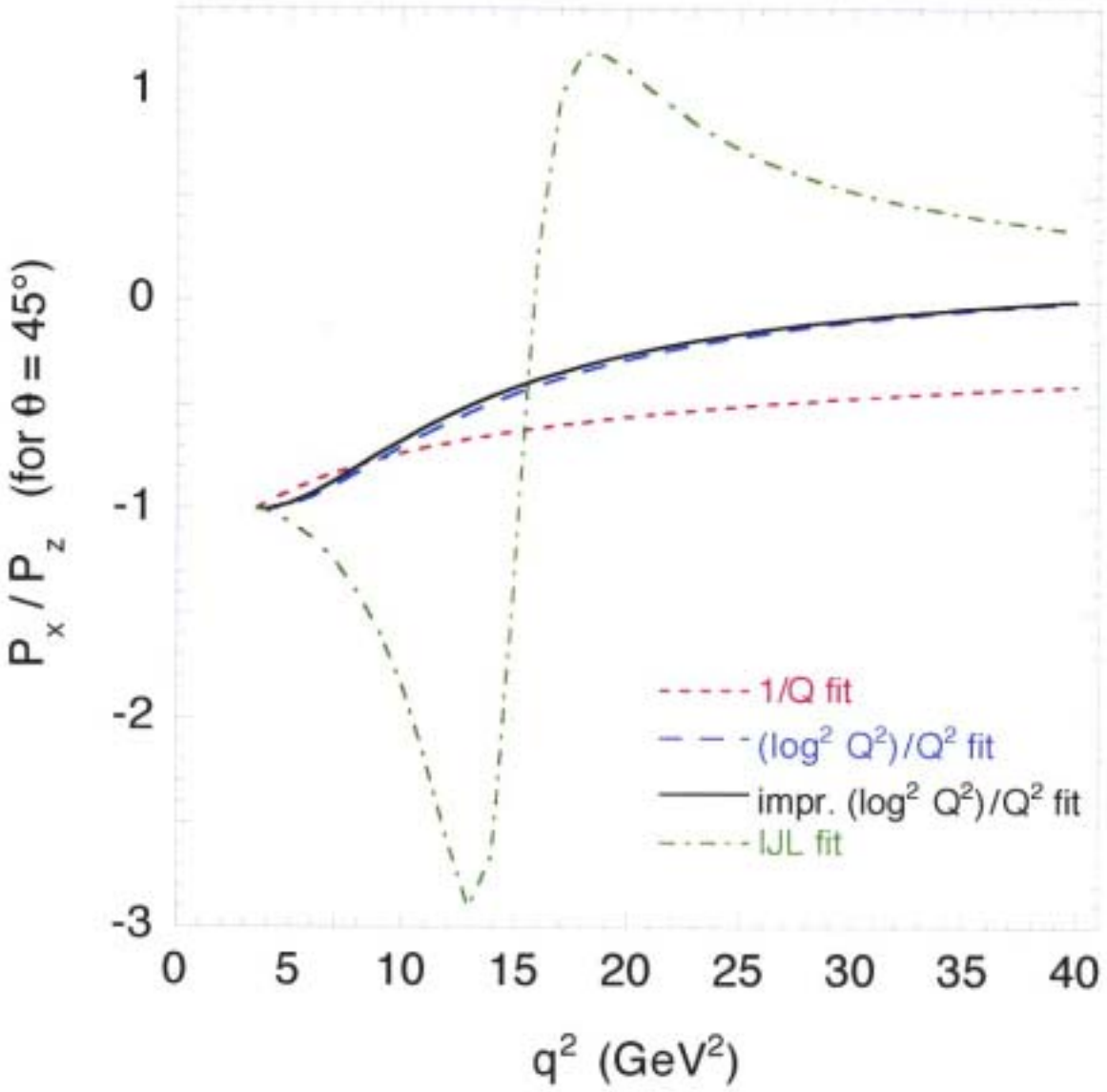
1
0
-1
-2
-3
0
5
10
15
20
25
30
35
40
P_x / P_z (for $\theta = 45°$)
q^2 (GeV^2)
1/Q fit
$(\log^2 Q^2)/Q^2$ fit
impr. $(\log^2 Q^2)/Q^2$ fit
IJL fit

BCHH

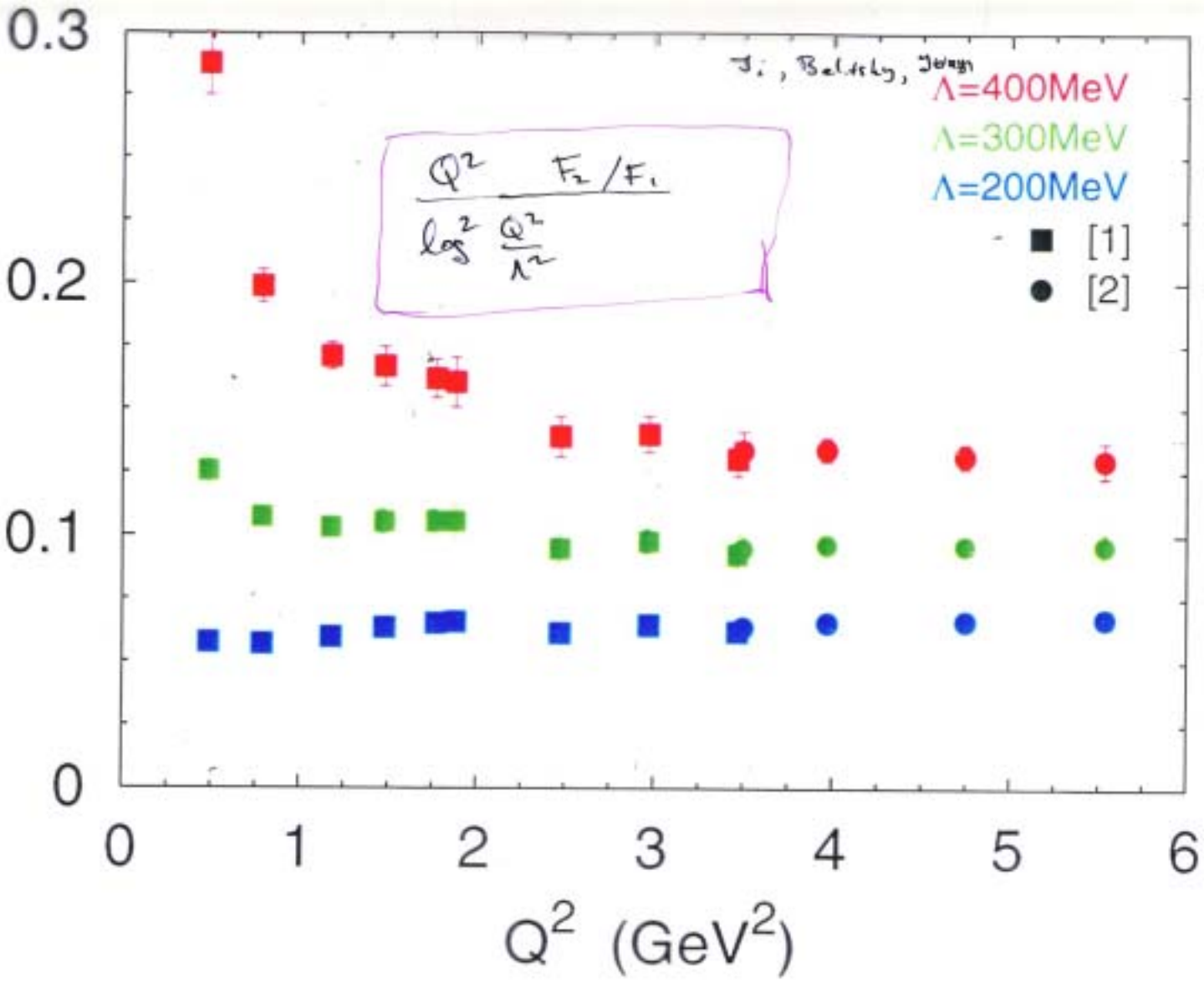
0.3
0.2
0.1
0
0
1
2
3
4
5
6
Q^2 (GeV^2)
Λ=400MeV
Λ=300MeV
Λ=200MeV
[1]
[2]
Q^2 F_2/F_1
$\log^2 \frac{Q^2}{\Lambda^2}$

J. Hiller
D.S. Huang
SJB

PQCD - Motivated Fit to JLAB Data

$$\frac{F_2(Q^2)}{F_1(Q^2)} = \frac{M_A}{1 + \frac{Q^2}{0.96\ \text{GeV}^2} \log^b\left(1 + \frac{Q^2}{4m_\pi^2}\right)}$$

$$M_A = 1.79$$

$$b = -0.6$$

$$q^2 = t = -Q^2$$

$Q^2 \to \infty$:

$$\frac{Q^2 F_2(Q^2)}{F_1(Q^2)} \sim \log^{0.6} Q^2$$

consistent with PQCD and hadron-helicity conservation

$$\frac{F_2(Q^2)}{F_1(Q^2)} = \frac{M_A}{1 + \frac{Q^2}{.96\,\text{GeV}^2}\log^{-.6}\left(1 + Q^2/4M_\pi^2\right)}$$

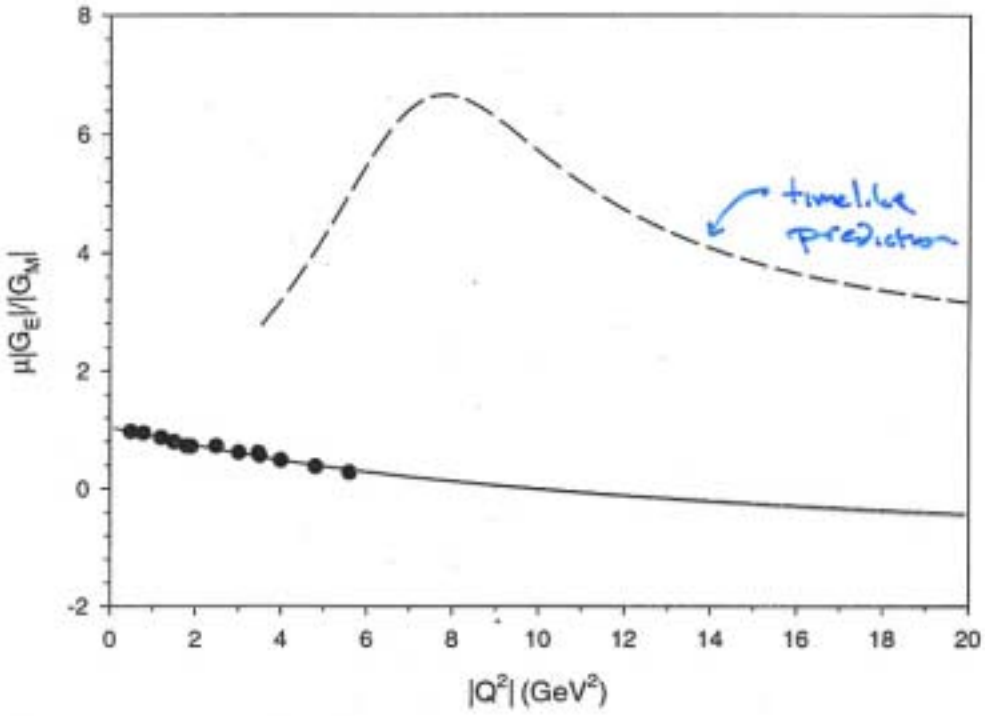

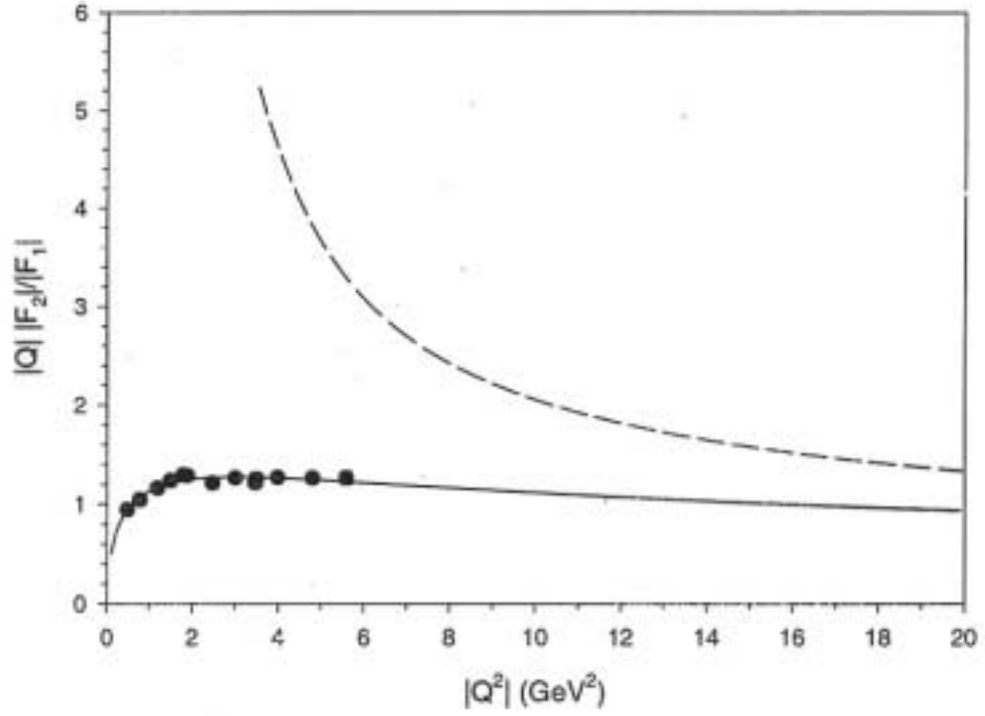

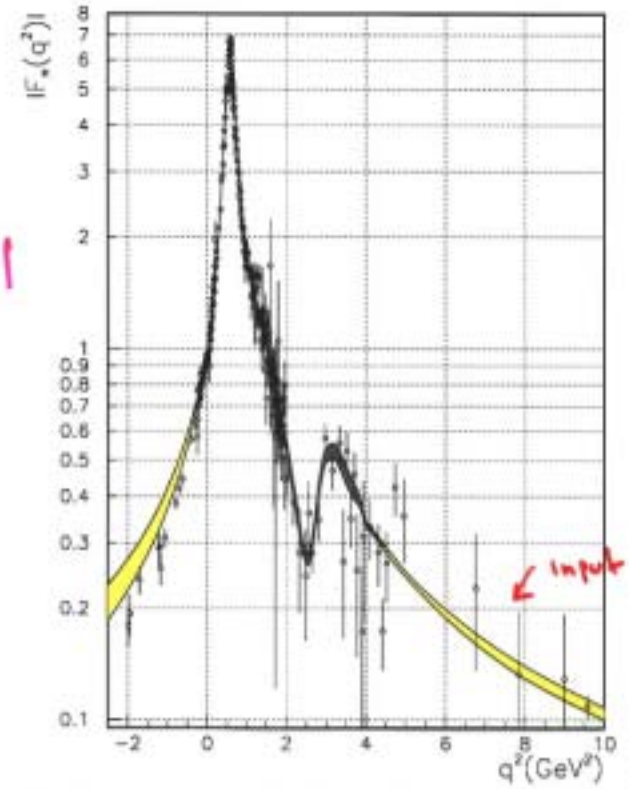

Fig. 2. Pion form factor. The black shaded area is the solution of (6), the gray shaded area is the input of the equation

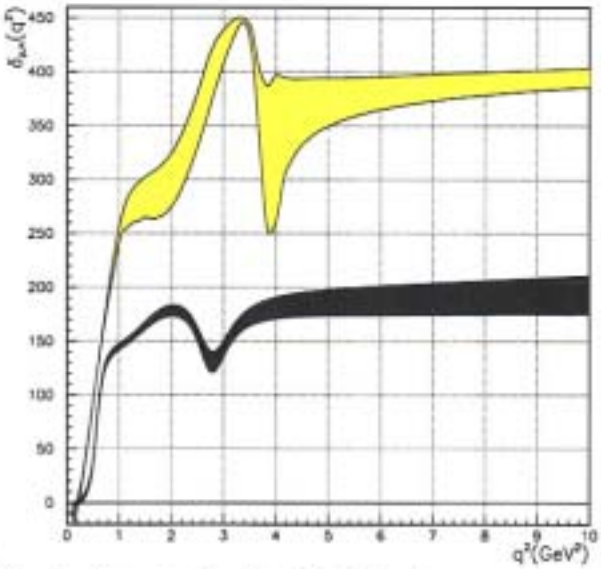

Fig. 3. Phase of pion (black shaded) and proton magnetic (gray shaded) form factor according to (2)

conclusion, in the whole range explored, what is actually measured is very likely to be G_M.

G_M^n seems to reach its expected asymptotic behavior $1/Q^4$ quite precociously, but it is higher by a factor of 2 than G_M^n at the same space-like $|Q^2|$, whereas asymptotically, they should be equal [23]. Therefore, an asymptotic extrapolation done according to PQCD may be suspect. Yet it has been checked that all the achieved results are quite insensitive to the details of this extrapolation.

Very near threshold, the data show a steep variation [15], beyond Coulomb enhancement (which has already been corrected in the data). In the following, this steep rise has been assumed to affect the FF in a limited Q^2 region, below and above the threshold. This is the reason for choosing $Q_2^2 = 4M_N^2 + \Delta$ as upper limit in (3). G_M and the first two derivatives are supposed to be continuous functions through this upper limit.

Once a FF G_0 has been determined from (6), another DR is considered in the interval $[Q_1^2 - \Delta, Q_1^2 + \Delta]$:

$$\frac{Q^2}{\pi}\int_{Q_1^2-\Delta}^{Q_1^2}\frac{\log|G_1(t)|}{t(t-Q^2)\sqrt{t-Q_0^2}}\mathrm{d}t + \frac{Q^2}{\pi}\int_{Q_1^2}^{Q_1^2+\Delta}\frac{\log|G_1(t)|}{t(t-Q^2)\sqrt{t-Q_0^2}}\mathrm{d}t = 0 \quad (7)$$

where G_1 is determined from the relation: $G_M = G_0 G_1$ in this interval and $G_M = G_0$ outside. Finally, the proton magnetic FF in the unphysical region as obtained by our procedure is reported in Fig. 4a.

The most striking feature of Fig. 4a is the evidence for two resonances, not built in *a priori*, at $M \sim 770$ MeV and $M \sim 1600$ MeV. It is most satisfying to deduce the presence of $\rho + \omega$ and of $\rho' + \omega'$ exactly as expected. On the other hand, the width of the bump at the ρ mass is ~ 350 MeV, to be compared to $\Gamma_\rho \sim 150$ MeV. Old analyses of the nucleon FF had already found a similar discrepancy [2].

The anomalous width, mainly related to the real part, turns out to be independent of the choice of the τ parameter within an order of magnitude. It cannot be due to the bin width, whose contribution is added quadratically and is relatively small in the ρ case. On the other hand, as was mentioned previously, the ρ width was recovered in the case of the pion FF.

Concerning the strange, polarized content of the nucleon, there is no evidence of a bump at the Φ mass, even if integrated on the bin width. If indeed the strange content of the nucleon is $\int \mathrm{d}Q^2(|G_M^s|/|G_M|)^2 \sim 0.15 \div 0.2$, it should be quite visible, concentrated mainly in the Φ mass bin. However, for a more quantitative statement to be made, the anomalous ρ width should be understood.

In Fig. 3, the phase of the proton magnetic FF is shown, the spectral function and other plots are reported elsewhere [31]. Above ~ 2 GeV, the phase is ~ 390 degrees, to be compared to the expected asymptotic value of 360 degrees [27].

In Fig. 1b the proton space-like magnetic FF data are compared with the expectation from the solution of the DR on $\log G(Q^2)$. The hypothesis there are no zeros on